JOURNAL OF CATALYSIS 45, 339–348 (1976)

A Molecular Orbital Investigation of the Wacker Process for the Oxidation of Ethylene to Acetaldehyde

D. R. ARMSTRONG, R. FORTUNE, AND P. G. PERKINS

Department of Pure and Applied Chemistry, University of Strathclyde, Glasgow G1 1XL, Scotland, U.K.

Received May 21, 1976

The oxidation of ethylene to acetaldehyde in the presence of $[PdCl_4]^{2-}$ has been studied using a CNDO-based method. A new reaction path is postulated involving the intermediate complex $[C_2H_4PdCl_3]^-$. The reaction sequence is initiated by the introduction of a water molecule at each of the available coordination sites of the metal perpendicular to the plane of the ethylene palladium trichloride anion. The chloride ligand *trans* to the coordinated ethylene is displaced by an entering water molecule. The departing halide extracts a proton from the second water and the generated hydroxyl ligand reacts with the ethylene, while remaining in the coordination sphere of the metal. This rate-determining step yields a β-hydroxyethyl palladium species as an intermediate and this can transform by a series of hydrogen shifts into a weak complex of acetaldehyde and palladium(0). Reasons are presented for the greater catalytic efficiency of $[PdCl_4]^{2-}$ relative to $[PtCl_4]^{2-}$ and for the inability of nickel and titanium complexes to catalyze the reaction.

INTRODUCTION

In recognition of the industrial importance of metal-catalyzed olefin oxidation reactions, considerable attention has, in recent years, been focused on this aspect of transition-metal chemistry (*1–3*). The foremost of these reactions is the Wacker process (*4*), in which an olefin is converted to its corresponding aldehyde or ketone in the presence of a palladium chloride catalyst. As a result of numerous systematic studies (*5–12*), primarily designed to elucidate the mechanism of this reaction, the gross features of the process are now well established and the reaction scheme proposed by Henry (*8, 9*) has gained wide acceptance. However, in contrast with the abundance of experimental detail available, data concerning the distribution of electrons pertinent to this reaction remain decidedly scant. A recent paper has partially alleviated this deficit (*13*) but, in order to advance the topic further, a molecular orbital investigation of the entire process was undertaken in order to gain a better understanding of the mechanisms involved.

The reasons for the superior catalytic activity of palladium and the inability of first-row transition metals to promote the reaction were also examined theoretically. This was achieved by explicit consideration of reaction sequences involving platinum, nickel, and titanium in place of palladium.

REACTION SCHEMES

The Henry mechanism of the Wacker process is sketched in Fig. 1. Under the operating conditions of the reaction, palladium is present initially as $[PdCl_4]^{2-}$ and this reacts with ethylene and then water to give $[C_2H_4PdCl_2H_2O]$. Ionization of the coordinated water molecule generates a hydroxyl ligand which then undergoes a *cis*-insertion reaction to produce a β-hy-

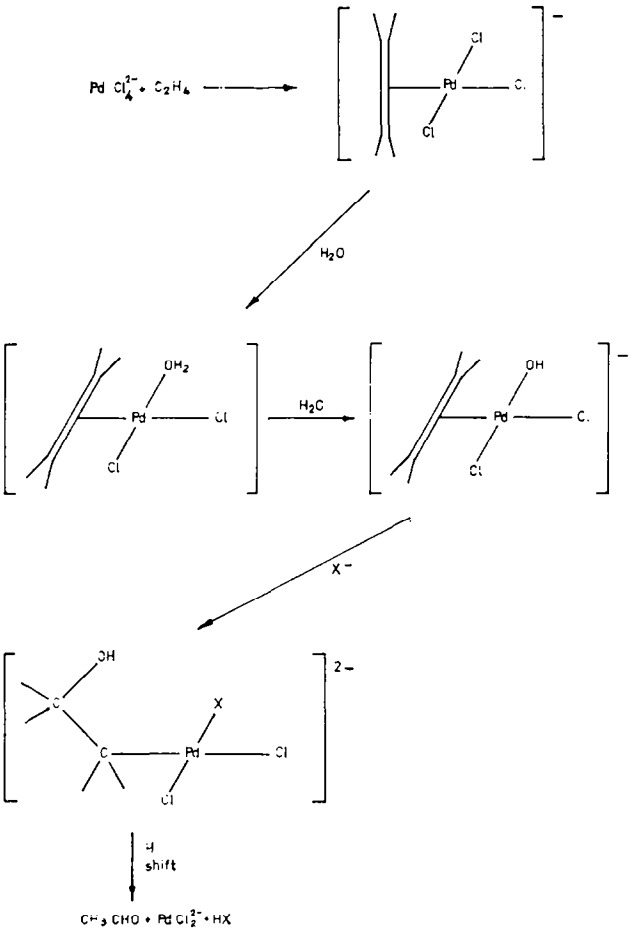

FIG. 1. Reaction scheme of Henry; X^- is chloride ion or solvent.

droxyethyl palladium species. This intermediate is then transformed, by a series of hydrogen shifts, to acetaldehyde and palladium in its zeroth oxidation state.

The reaction sequence outlined above is based on the assumption that the ethylene and the hydroxide ion will achieve a *cis*-orientation in the square-planar palladium complex. This is somewhat contrary to current chemical thinking, which designates ethylene as a strong *trans*-directing ligand (*14*). The existence of the *cis*-isomer has been rationalized latterly (*1*) either by the occurrence of *trans* to *cis* isomerization or by the presence of kinetically significant amounts of the *cis*-compound. In our view, however, neither reason can completely justify the presence of the *cis*-isomer in the reaction scheme. In response to this dilemma, we propose an initial reaction process involving the *trans*-isomer.

In square-planar complexes, the substitution of a ligand proceeds via a distorted trigonal-bipyramidal intermediate (*15*, *16*). A modified variant of this structure is envisaged here. The square-planar complex $[C_2H_4PdCl_3]^-$ generated *in situ* has solvent sites available above and below the molecular plane. These may be occupied by solvent water molecules, resulting in a complex of type B shown in Fig. 2. A concerted rate-determining reaction sequence then ensues. The chloride ligand *trans* to the coordinated ethylene is displaced by an entering water

molecule following a reaction path which involves a distorted trigonal bipyramidal intermediate shown in Fig. 3. The departing chloride ligand extracts a proton from the second water molecule and hydrogen chloride leaves the coordination sphere of the metal. The remaining hydroxide moiety remains bonded to the metal and this facilitates nucleophilic attack on the ethylene, promoting the formation of a carbon–oxygen bond and the generation of complex C.

The remaining stages of the reaction scheme involve two hydrogen shifts and a reduction in the formal oxidation state of palladium from two to zero. The oxygen–hydrogen bond is broken and the hydrogen leaves the palladium complex while a hydrogen bonded to the enolic carbon transfers to the neighbouring carbon atom. We make the simplifying assumption that the departing hydrogen atom combines with a coordinating chlorine atom and exits as HCl. In practice the exiting proton may

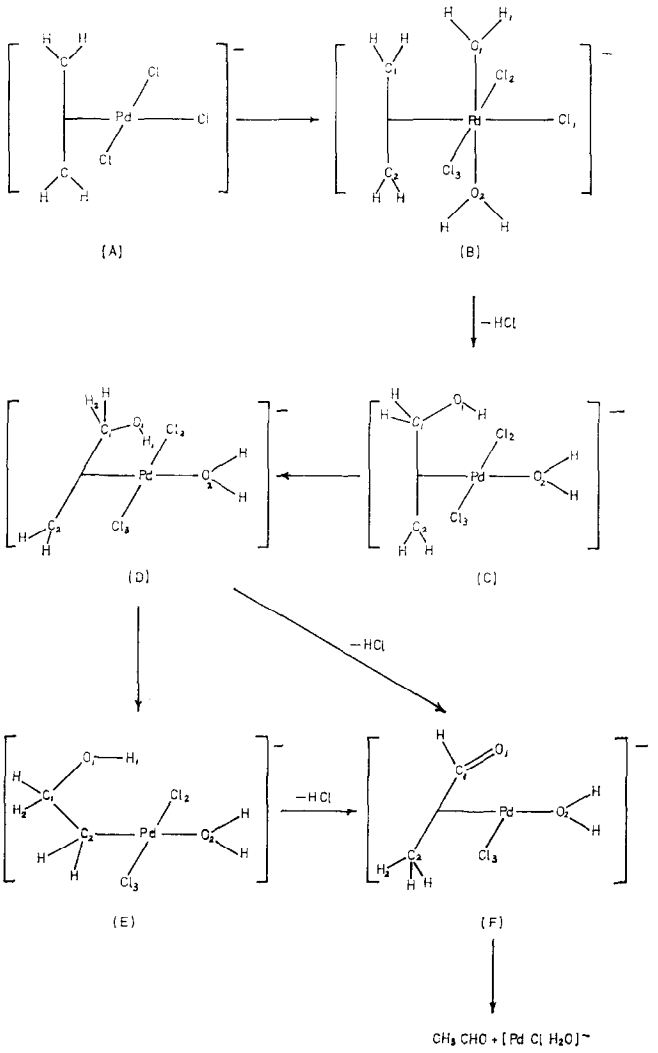

FIG. 2. Modified reaction scheme for the Wacker process.

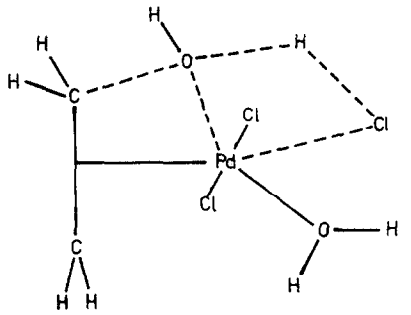

FIG. 3. The distorted trigonal bipyramidal intermediate of reaction sequence B → C.

be solvated or attached to a free chloride ion; however, the postulated reaction path was adopted for computational convenience. In order to obtain the essential chlorine–hydrogen interaction, it is necessary to rotate the hydroxyethylene component into the same plane as the palladium dichloride unit, producing complex D of Fig. 2. There are two possible ways by which the intramolecular hydrogen shift may then occur. Firstly, by direct rearrangement to a product F where the acetaldehyde is loosely bound to the palladium metal or secondly, by geometrical reorganization to the intermediate β-hydroxyethyl palladium species, E, which then transforms to the final product, F.

CALCULATIONAL METHOD

The calculations were performed within a slightly modified CNDO framework, as described previously (*17*, *18*) and successfully applied to platinum complexes (*16*). Our approach was to examine the electronic structure of intermediates at selected points along the reaction coordinate. The quantities of particular interest are the electron densities and the bond indices (*19*, *20*) defined by

$$B_{AB} = \sum_{\lambda \text{ on A}} \sum_{\sigma \text{ on B}} P_{\lambda\sigma}^2,$$

where $P_{\lambda\sigma}$ is a density matrix element. The bond index B_{AB} is a useful measure of the bonding between atoms A and B, since it directly indicates the multiplicity of the bond, e.g., the C–C bond indices (*20*) in C_2H_6, C_2H_4, and C_2H_2 are calculated to be ~1, ~2, and ~3, respectively.

In the construction of a reaction path, the ideal procedure would be to calculate the total energy of the intermediate at all points on the reaction surface. This is impractical for systems with many degrees of freedom and, in any case, semiempirical methods such as CNDO do not afford absolute energies. Hence, we did not attempt to calculate the activation energy directly. We have, instead, used chemical intuition to construct plausible reaction paths for each process. All bond lengths and angles were obtained from Ref. (*21*). The relevant input data for all the atoms except palladium have been published previously (*22*). The diagonal elements for palladium of the core Hamiltonian matrix were equated to the corresponding valence orbital ionization potentials (*23*), while the value of the one-center, two-electron, repulsion integrals for the *s*, *p*, and *d* orbitals of palladium was 7.2 eV.

RESULTS AND DISCUSSION

Reaction Sequence B → C: Formation of the C–O bond

The electron distributions calculated at six points along the postulated reaction path are recorded in Table 1. Inspection of the electron populations of complex B reveals that the solvent water molecules are weakly bound to the palladium and the number of electrons transferred to the central metal ion amounts to only 0.03e/water molecule. Hence, the electronic structure of the initial ethylene complex is not radically altered by solvation. It is found that there is an overall transfer of electronic charge to the ethylene. The olefinic π and π* orbitals, traditionally considered to be involved in synergic metal–ethylene bonding, are occupied by 1.72 and 0.36 electrons, respectively, and these values, in conjunction with the large Pd–C bond indices, con-

firm that significant interaction occurs between ethylene and palladium.

As the reaction proceeds, the C–O bond is formed at the expense of Pd–C and C–C bonding. The Pd–C_1 interaction becomes virtually nonbonding and a decline in the double-bond character of the coordinated ethylene is evident. The decrease in the calculated stability of the species during the reaction sequence can be correlated with the overall reduction in the bonding interactions. It is encouraging to note that the identification of this reaction step as rate-determining agrees with experimental inference. The comparatively small activation energy, which demonstrates the feasibility of this postulated reaction profile, may be attributed to the gain in energy due to C_1–O_1 and Pd–O_1 bond formation almost equalling the energy loss entailed in the weakening of C–C and Pd–C bonds. The formation of strong Pd–O bonding during the reaction sequence reflects the relative donor capabilities of hydroxyl and water as ligands.

The regulating function of the metal *d* orbitals is readily apparent during the aforementioned reorganization of bonding interactions over the reaction coordinate. At the beginning of the reaction sequence, the metal d_{z^2} orbital assumes the principal bonding role to the oxygen. The electron occupancy of this orbital approaches saturation at the early stages of the postulated reaction path. Consequently, this metal orbital does not participate extensively in the bonding and hence, an initial low Pd–O bond index is obtained despite the favorable orbital orientations. As the reaction proceeds, the oxygen enters the domain of the metal d_{xz} orbital and so remains in the coordination sphere of the palladium. This control exerted by the *d* orbitals continues as the oxygen enters the immediate environment of the carbon atom. The strong Pd–O and Pd–C_2 bonding present in the intermediate moiety C is due principally to the metal d_{xz} orbital which, freed from bonding to C_1, is able to participate more extensively in bonding to these ligand atoms.

Of particular interest is the accumulation of excess electron density on C_2 concomitant with the destruction of the double-bond character of ethylene. The additional elec-

TABLE 1

Electronic Distribution over the Reaction Coordinate B → C

Step	Pd	Cl_1	Cl_2	O_1	O_2	C_1	C_2	H_1
Atom charges								
B 1	+0.237	−0.459	−0.547	−0.253	−0.253	−0.034	−0.034	+0.143
2	+0.289	−0.584	−0.530	−0.110	−0.248	−0.023	−0.030	−0.021
3	+0.423	−0.437	−0.522	−0.302	−0.240	+0.005	−0.068	−0.075
4	+0.456	−0.167	−0.570	−0.433	−0.210	+0.070	−0.218	+0.057
5	+0.479	−0.105	−0.596	−0.369	−0.221	+0.115	−0.341	+0.119
C 6	+0.448	−0.150	−0.716	−0.203	−0.242	+0.141	−0.300	+0.150

Bond indices									
Step	Pd–Cl_1	Pd–Cl_2	Pd–O_1	Pd–O_2	Pd–C_1	Pd–C_2	C_1–C_2	C_1–O_1	H_1–Cl_1
B 1	0.780	0.682	0.050	0.050	0.241	0.241	1.768	0.002	0.000
2	0.592	0.731	0.084	0.068	0.274	0.275	1.713	0.017	0.025
3	0.255	0.763	0.165	0.124	0.266	0.283	1.628	0.110	0.366
4	0.120	0.734	0.223	0.213	0.186	0.178	1.436	0.329	0.822
5	0.039	0.724	0.251	0.178	0.126	0.146	1.165	0.552	0.977
C 6	0.019	0.582	0.503	0.078	0.074	0.384	1.060	0.715	0.975

tron population is located in the p_x orbital and, as this lies in the path of the migrating hydrogen, the ultimate formation of a C_2–H bond is facilitated.

Reaction Sequence C → D: Rotation of the Hydroxyethylene Species about the Metal–Ethylene Bond

In this reaction step, the hydroxyethylene moiety is rotated about the metal–ethylene axis so that it is in the same plane as the $[PdCl_2(OH_2)]$ unit. A simultaneous rotation of the coordinated olefin about the carbon–carbon axis positions the migrating hydrogen in the same plane as the Pd–ethylene plane. Dramatic changes in the electron distribution accompany these postulated rotations: thus, the Pd–C_2 bond is reinforced while the Pd–O_1 bond is weakened during the reaction step. This latter interaction, which promoted initial formation of the C–O bond, would now hinder the ensuing hydrogen transfer. The energetics of this reaction step show that the rotational changes produce an overall gain in stability of the system. Consequently, we postulate that this rotation is a plausible occurrence in the Wacker process and, indeed, may occur isochronally with the rate-determining step.

Nature of the Hydrogen Shifts

Path I. Reaction sequence D → F. The exact routes taken by the migrating hydrogen atoms are, of course, unknown. The path adopted by the intramolecular hydrogen shift is expected to be influenced by both C–H and Pd–H interactions and therefore, in the preliminary studies of this stage of the reaction, two migratory routes were investigated. In route (i) the hydrogen-to-palladium distance is kept constant throughout the transfer, while in route (ii) the Pd–H distance is varied at chosen intermediate points so as to give a maximum Pd–H bond index.

The calculations reveal that for route (i) the C–H interaction controls the migration, while the Pd–H interaction is negligible. The longer Pd–H distances in route (ii) allow the diffuse metal orbitals to play an important role and so the C–H interactions are of secondary importance. In route (i) the charge on the migrating hydrogen remains essentially zero, while in route (ii) the hydrogen carries a negative charge. A more realistic reaction path is more likely to embody both Pd–H and C–H interactions and hence route (iii) was constructed: here the Pd–H distance was maintained as the arithmetic mean of the Pd–H distances used in routes (i) and (ii).

The atom charges and bond indices of the intermediate structures at various points of route (iii) are presented in Table 2. The overall effects are similar to those of routes (i) and (ii). As the reaction proceeds, there is an increase in electron density on the Pd and this accumulates especially in the $d_{x^2-y^2}$ orbital. This build-up of charge is consistent with the observed chemical reduction of Pd in the catalytic process. Considerable electron density is transferred from the leaving chlorine atom to the metal, as the H–Cl bond is formed. Both carbon atoms lose a small amount of electron density during the course of this reaction sequence. For C_1 this is due to the formation of the C_1–O double bond, while for C_2 the greatly reduced interaction with palladium is a major reason for electron withdrawal. The intramolecular migrating hydrogen gains electron density, attaining its maximum negative charge at the midpoint of the hydrogen shift. The variation in Pd–H interactions correlates well with the electron density changes on the hydrogen, thus identifying Pd as the donor of the extra electronic charge. The most important single component of the Pd–H bond is the in-plane interaction of the hydrogen with the Pd $d_{x^2-y^2}$ orbital. An interesting point about the hydrogen migration is that the sum of C–H interactions reaches a

TABLE 2

The Electronic Distribution over the Reaction Coordinate D → F

Step	Pd	Cl_2	Cl_3	O_1	O_2	C_1	C_2	H_1	H_2
Atom charges									
D 1	−0.298	−0.796	−0.396	−0.265	−0.194	+0.180	−0.202	+0.198	−0.011
2	−0.413	−0.748	−0.413	−0.270	−0.194	+0.188	−0.010	+0.262	−0.043
3	−0.501	−0.738	−0.444	−0.275	−0.192	+0.251	+0.013	+0.271	−0.067
4	−0.576	−0.367	−0.527	−0.317	−0.189	+0.272	+0.022	+0.217	−0.184
5	−0.642	−0.218	−0.602	−0.302	−0.187	+0.264	−0.004	+0.183	−0.150
6	−0.659	−0.129	−0.653	−0.246	−0.182	+0.218	−0.038	+0.154	−0.075
F 7	−0.633	−0.136	−0.673	−0.369	−0.182	+0.145	−0.115	+0.153	+0.036
Bond indices									
	Pd–Cl_2	Pd–Cl_3	Pd–O_1	Pd–O_2	Pd–C_1	Pd–C_2	C_1–C_2	C_1–O_1	
D 1	0.643	0.571	0.030	0.084	0.081	0.560	1.051	0.947	
2	0.512	0.543	0.040	0.106	0.093	0.465	1.064	0.983	
3	0.349	0.503	0.048	0.115	0.129	0.332	1.090	1.050	
4	0.141	0.528	0.079	0.116	0.139	0.200	1.096	1.398	
5	0.082	0.593	0.088	0.115	0.129	0.154	0.071	1.721	
6	0.050	0.636	0.096	0.111	0.127	0.103	1.031	1.828	
F 7	0.032	0.652	0.062	0.111	0.113	0.096	1.056	1.835	
	O_1–H_1	Cl_2–H_1	Pd–H_2	C_1–H_2	C_2–H_2				
D 1	0.917	0.000	0.016	0.917	0.006				
2	0.870	0.024	0.077	0.809	0.041				
3	0.734	0.126	0.089	0.644	0.135				
4	0.215	0.678	0.108	0.277	0.362				
5	0.046	0.931	0.062	0.099	0.651				
6	0.001	0.961	0.046	0.035	0.830				
F 7	0.000	0.971	0.033	0.022	0.883				

minimum at the midpoint of the reaction path. Hence, we observe that the palladium atom aids the hydrogen shift by bonding to it at positions where the carbon–hydrogen bonding is at a minimum.

Path II. Reaction sequence D → E → F. There are only minor changes in the electron distribution for the reaction sequence D → E. The formation of the β-hydroxyethyl palladium species, E, involves a further weakening of the Pd–C_1 bond, while the Pd–C_2, C–O and the Pd–Cl bonds are reinforced (Table 3).

The second part of this reaction sequence involves the two hydrogen shifts for which the reaction paths were obtained by the procedure used for Path I. Comparison of the electron distribution changes with those in Table 2 reveals that they are very similar (although, for brevity, we do not detail them here). The only essential difference between the two processes is that in Path II the palladium does not lie on the perpendicular bisector of the C_1–C_2 bond and so in the hydrogen migration, the C–H interactions are not as symmetrical as they are in Path I.

Comparison of Paths I and II

From bonding considerations, it is very difficult to determine which of the above reaction sequences provides a better description of the hydrogen shift mechanism.

TABLE 3

Electronic Distribution over the Reaction Coordinate D → E → F

Step	Pd	Cl_2	Cl_3	O_1	O_2	C_1	C_2	H_1	H_2
Atom charges									
D 1	−0.298	−0.796	−0.396	−0.265	−0.194	+0.180	−0.202	+0.198	−0.011
E 2	+0.052	−0.551	−0.560	−0.299	−0.213	+0.096	−0.115	+0.153	−0.002
3	−0.096	−0.669	−0.503	−0.323	−0.209	+0.163	−0.053	+0.229	−0.046
4	−0.278	−0.741	−0.488	−0.261	−0.203	+0.221	0.000	+0.208	−0.049
5	−0.511	−0.501	−0.529	−0.279	−0.192	+0.268	+0.052	+0.179	−0.119
6	−0.658	−0.137	−0.613	−0.298	−0.182	+0.233	+0.027	+0.139	−0.101
7	−0.666	−0.110	−0.648	−0.254	−0.182	+0.215	−0.027	+0.135	−0.063
F 8	−0.633	−0.136	−0.673	−0.369	−0.182	+0.145	−0.115	+0.153	+0.036

Bond indices

	Pd–Cl_2	Pd–Cl_3	Pd–O_1	Pd–O_2	Pd–C_1	Pd–C_2	C_1–C_2	C_1–O_1
D 1	0.634	0.571	0.030	0.084	0.081	0.560	1.051	0.947
E 2	0.685	0.705	0.026	0.109	0.045	0.769	1.017	0.952
3	0.555	0.704	0.021	0.106	0.074	0.779	1.036	0.989
4	0.422	0.675	0.028	0.108	0.099	0.654	1.069	1.031
5	0.187	0.638	0.040	0.113	0.091	0.359	1.126	1.291
6	0.084	0.652	0.061	0.112	0.091	0.152	1.061	1.701
7	0.053	0.653	0.079	0.111	0.108	0.108	1.038	1.833
F 8	0.032	0.652	0.062	0.111	0.113	0.096	1.056	1.835

	O_1–H_1	Cl_2–H_1	Pd–H_2	C_1–H_2	C_2–H_2
D 1	0.917	0.000	0.016	0.917	0.006
E 2	0.929	0.013	0.038	0.936	0.003
3	0.909	0.013	0.073	0.853	0.023
4	0.868	0.037	0.104	0.712	0.090
5	0.426	0.469	0.128	0.368	0.309
6	0.033	0.920	0.059	0.124	0.674
7	0.001	0.967	0.042	0.040	0.831
F 8	0.000	0.971	0.033	0.022	0.883

When the total energies are inspected, however, we find that there are significant differences in the energetics of Paths I and II. Although both reaction sequences bring about increased stability of the system, the formation of a β-hydroxyethyl palladium species is especially favoured. This can be explained by recalling that, for the intermediate D, there is only one significant Pd–C bond and therefore retention of the assumed isosceles triangular shape for the palladium–carbon–carbon unit is no longer necessary. The sequence D → E may be considered as an optimization of the geometry of D involving minimization of the nuclear energy and so producing a decrease in total energy.

Examination of the total energy calculated for Path II reveals that an energy minimum occurs when the hydrogen shift is half-complete. This suggests that our postulated reaction path should be slightly modified in the direction of a more loosely bound complex at this point. This is confirmed by further calculations which produce an energy minimum on completion of the hydride shift. In these calculations the palladium–hydrogen interactions become

even more important at the midpoint of the hydrogen shift, as at this position both C–H interactions have become very small.

The forcing conditions required for olefin oxidation in the presence of the comparable platinum(II) tetrachloride anion may be attributed to a number of factors. Consideration of the electronic structure of the initial complex A reveals that the palladium species is more amenable to the changes required by the process than the platinum analogue. The bond indices between platinum and the olefinic carbon atoms are significantly larger than the corresponding values pertaining to palladium, due to the more marked ability of platinum to partake in σ–π synergic bonding (*24*). The resulting increase in the electron occupancy of the olefinic π^* orbital requires the nucleophilic hydroxide ion to attack a position of greater electron density. Furthermore, the stronger platinum–carbon bonds make the electronic redistribution, necessary for the new bonding patterns, rather more difficult.

The calculation of hydrogen shift sequences from complex D to F was repeated with platinum, nickel and titanium in place of palladium. It was found that the hydrogen-transfer processes were energetically favourable irrespective of the central ion employed. Consequently, the inability of nickel and titanium compounds to act as catalysts in the Wacker process is most probably due to the nonformation of the nickel and titanium analogues of Zeise's anion. This is a consequence of the unfavourable geometries adopted by $NiCl_4^{2-}$ and $TiCl_4$ which have D_{2d} and T_d symmetry, respectively, in contrast to the D_{4h} symmetry of $PdCl_4^{2-}$ and $PtCl_4^{2-}$.

In conclusion, the Wacker process occurs in two distinct stages. The first entails the formation of a carbon–oxygen bond and is rate-determining. The second step involves the reorganization of the hydroxyethylene palladium species to produce acetaldehyde loosely bound to palladium in its zeroth oxidation state through a sequence of hydrogen shifts. Palladium is an essential component of the first stage by allowing the formation of a complex with ethylene and water to occur. In this intermediate the synergic bounding between palladium and ethylene is necessary to weaken the olefinic bond. Transient Pd–O bonding enhances formation of the C–O bond by restricting the nucleophilic hydroxyl species to the coordination sphere of the metal. During the final stage of the reaction, the *d* orbitals of the palladium assist the intramolecular migration of the hydrogen.

ACKNOWLEDGMENT

One of us (R. F) thanks the University of Strathclyde for a Crawford Bursary.

REFERENCES

1. Maitlis, P. M., "The Organic Chemistry of Palladium." Academic Press, London, 1971.
2. Hartley, F. R., "The Chemistry of Platinum and Palladium." Appl. Sci. Publ., London, 1973.
3. Aquilo, A., *Advan. Organomet. Chem.* **5**, 321 (1967).
4. Smidt, J., *Chem. Ind.* **1962**, 54.
5. Smidt, J., Hafner, W., Jira, R., Sieber, R., Sedlmeier, J., and Sabel, A., *Angew. Chem. Int. Ed.* **1**, 80 (1962).
6. Moiseev, I. I., Vargaftik, M. N., and Syrkin, Y. K., *Dokl. Akad. Nauk.*, **153**, 140 (1960).
7. Moiseev, I. I., Vargaftik, M. N., and Syrkin, Y. K., *Dokl. Akad. Nauk* **171**, 1365 (1966).
8. Henry, P. M., *J. Amer. Chem. Soc.* **86**, 3246 (1964).
9. Henry, P. M., *J. Amer. Chem. Soc.* **88**, 1595 (1966).
10. Moiseev, I. I., Vargaftik, M. N., Pestrikov, S. V., Levanda, O. G., Romanova, T. N., and Syrkin, Y. K., *Dokl. Akad. Nauk* **171**, 1365 (1966).
11. Henry, P.M., *J. Amer. Chem. Soc.* **94**, 4437 (1972).
12. Moiseev, I. I., Levanda, O. G., and Vargaftik, M. N., *J. Amer. Chem. Soc.* **96**, 1003 (1974).
13. Sakaki, S., Kato, H., Kanai, H., and Tarama, K., *Bull. Chem. Soc. Japan.* **47**, 377 (1974).
14. Bersuker, I. B., *Russ. J. Inorg. Chem.* **18**, 9 (1964).
15. Chatt, J., Duncanson, L. A., and Venanzi, L. M., *J. Chem. Soc.* **1966**, 4456.
16. Armstrong, D. R., Fortune, R., and Perkins, P. G., *Inorg. Chim. Acta* **9**, 9 (1974).

17. Pople, J. A., Santry, D. P., Segal, G. A., *J. Chem. Phys.* **43**, S129 (1965).
18. Armstrong, D. R., Perkins, P. G., and Stewart, J. J. P., *J. Chem. Soc.* (*A*), **1971**, 3654.
19. Armstrong, D. R., Perkins, P. G., and Stewart, J. J. P., *J. Chem. Soc. Dalton* **1973**, 838.
20. Armstrong, D. R., Perkins, P. G., and Stewart, J. J. P., *J. Chem. Soc. Dalton* **1973**, 2273.
21. "Tables of Interatomic Distances in Molecules and Ions." *Chem. Soc.*, London, Special Publ. No. 11 (1958).
22. Levison, K. A., and Perkins, P. G., *Theoret. Chim. Acta.* **14**, 206 (1969).
23. Moore, C. E., *Natl. Bur. Std.* (*U. S.*) Circ. No. 467 (1952).
24. Chatt, J., *J. Chem. Soc.* **1953**, 2939.